Structural stability of $NiTi_2$ intermetallic compounds

1993 J. Phys.: Condens. Matter 5 9087

(http://iopscience.iop.org/0953-8984/5/49/011)

J. Phys.: Condens. Matter 5 (1993) 9087–9098. Printed in the UK

Structural stability of $NiTi_2$ intermetallic compounds

D Nguyen Manh†‡, A Pasturel†, A T Paxton§ and M van Schilfgaarde§
† Laboratoire de Thermodynamique et de Physico-Chimie Métallurgiques, URA 29 CNRS, ENSEEG, BP 75, 38402 St Martin d'Heres, France
§ SRI International, 333 Ravenswood Avenue, Menlo Park, CA 94025, USA

Received 26 April 1993, in final form 2 September 1993

Abstract. For each of the compounds $MnTi_2$, $FeTi_2$, $CoTi_2$, $NiTi_2$, $PdTi_2$, $PtTi_2$ and $CuTi_2$, the differences between the total energies of the compounds in the $MoPt_2$-, $MoSi_2$- and $NiTi_2$-type crystal structures are calculated. Trends of structural energy differences are analysed by performing 'frozen-potential' energy difference calculations and site-projected-energy analysis. Our analysis reveals that the Ti sites with icosahedral symmetry determine the structural stability in transition metal (TM)–Ti_2 compounds. A connection with the stability of quasicrystal models is established.

1. Introduction

The transition metal–transition metal (TM–TM) compounds of the form TM–TM_2 form one of the most interesting classes of intermetallic compounds. For this composition, both geometrically and topologically close-packed structures may occur, emphasizing the different roles played by electronic effects and atomic-size effects in explaining the structural stability of such structures. According to a phenomenological analysis of the structural stability of topologically close-packed (TCP) structures [1], it is important to distinguish Laves phases from other TCP phases since the atomic-size ratio is essential in explaining the stability of the former. Among other TCP phases, the $NiTi_2$-type structure displays a peculiar behaviour since it is only partially tetrahedrally packed. The tetrahedral packing leads to characteristic polyhedra, which are labelled Z12, Z14, Z15 and Z16, where the numbers refer to the coordination number of the atom entering the polyhedron. The $NiTi_2$-type structure has three inequivalent site types, two of these sites (one Ti and one Ni) are icosahedrally coordinated (Z12), while the remaining site has 14 neighbours (see table 1). This structure occurs for $FeTi_2$, $CoTi_2$ and $NiTi_2$ compounds and has been extensively studied recently [2–4] since amorphous or quasicrystal phases can be formed by rapid-cooling methods in this composition range.

The purpose of this paper is to study the electronic and cohesive properties of the $NiTi_2$-type structure by using first-principles calculations based on the local density functional scheme, namely the linear-muffin-tin-orbitals method, including the combined correction terms in the atomic-sphere approximation (ASA). This study includes total energy calculations for the $NiTi_2$-type structure as well as for the two ordered $MoPt_2$- and $MoSi_2$-type structures. In fact, our strategy is made up of two levels: (i) to check the applicability of the ASA to the difficult problem concerning energy differences between different structures—this will be done by comparing ASA results with the ones provided by full potential

‡ Permanent address: Department of Physics, Polytechnic University of Hanoï, Vietnam.

0953-8984/93/499087+12$07.50

calculations; (ii) to use the facilities of ASA such as site-projected-energy analysis, the frozen-potential approach, and first-principles tight-binding parameters to obtain new physical insights into the structural stability of the three considered structures. In section 2, we present total energy calculations for the $NiTi_2$-type structure and for the two other ordered $MoPt_2$- and $MoSi_2$-type structures. A study of the relative structural stability among these three phases allows us to distinguish the energetically favourable and unfavourable sites for the $NiTi_2$-type structure. In section 3, a systematic study of the electronic density of states (DOS) of TM–Ti_2 compounds (TM = Mn, Co, Fe, Pd, Pt, Cu) is presented. More particularly, the evolution of the Fermi level as a function of the d-band filling of the TM is discussed. In section 4, we make a connection with tight-binding theory and discuss the stability of some quasicrystal models.

2. Total energy calculations

2.1. Description of structures

In table 1, we give a structural identification of the three structures (i.e. $MoPt_2$-, $MoSi_2$- and $NiTi_2$-type structures) studied in this paper. As can be seen from the table, the orthorhombic $MoPt_2$-type structure has been built as a superstructure of the FCC lattice while the tetragonal $MoSi_2$-type ($C11b$) structure resembles the body-centred cubic structure. For the $MoSi_2$-type structure, the value for c/a is close to the experimentally observed ratio in a compound with $\Delta Ne > 0$ ($\Delta Ne = N_A - N_B$; N_A and N_B are the average valence electron numbers of the A and B constituents, respectively [10]). There are two inequivalent sites (one Ti and one Ni) for each structure. In the $MoPt_2$-type structure, Ti has five Ni and seven Ti at $a\sqrt{2}/2$ distance while Ni has two Ni and ten Ti at the same distance, a being the lattice parameter. In the $MoSi_2$-type structure, Ti has four Ni and four Ti at $a1\sqrt{3}/2$ distance while Ni has eight Ti at the same distance. The $NiTi_2$-type structure is characterized by three different Wyckoff positions, Ni(e), Ti(c) and Ti(f). Ni(e) and Ti(c) have icosahedral symmetry while Ti(f) has 14 nearest neighbours. Ti(f) has four Ti(f) at $0.265a2$ and four other Ti(f) at $0.267a2$; two Ti(c) are at $0.257a2$ while two Ni(e) are at $0.231a2$ and two other ones at $0.256a2$, $a2$ being the lattice parameter of this structure; Ti(c) has six Ni(e) are at $0.220a2$ and six Ti(f) at $0.257a2$; Ni(e) has three Ti(f) at $0.231a2$ and three other ones at $0.256a2$; three Ni(e) are at $0.249a2$ and three Ti(c) at $0.220a2$. The three structures are also displayed in figure 1. For the $MoPt_2$-type and $MoSi_2$-type structures, we have emphasized that they can be obtained as superstructures of the FCC and BCC lattices, respectively. The complex structure displayed in figure 1(c), can be described in the following way:

(i) the Ti(f) atoms are located at the vertices of regular octahedra which are centred at the nodes of a diamond lattice (figure 2(a));

(ii) the Ni(e) atoms are located at the vertices of regular tetrahedra, the centres of which build a diamond unit cell shifted by the vector $\frac{1}{2}[001]$ with respect to the cell formed by the Ti(f) octahedra (figure 2(b));

(iii) the Ti(c) atoms are located at the vertices of regular tetrahedra surrounding Ni(e) tetrahedra (figure 2(c)).

Since the Ti(f) atoms define octahedral interstices, the complex $NiTi_2$-type structure is not a tetrahedrally close packed structure, as already mentioned in section 1.

Table 1. Structural identification of the three $MoPt_2$, $MoSi_2$ and $NiTi_2$ structures.

Structure	System	Space group	Atoms/ cell	Lattice parameters (au)	Atomic positions	Type of first-nearest neighbours
$MoPt_2$	Orthorhombic	$Immm$	6	$a = 7.418$ $b = a/\sqrt{2}$ $c = 3a/\sqrt{2}$	Mo2(a) (0,0,0) Pt 4(g) $(0,0,\frac{1}{3})$	Mo origin: 2Mo+10Pt Pt origin: 5Mo+7Pt
$MoSi_2$	Tetragonal	$I4/mmm$	6	$a = 5.707$ $c = 3.295a$	Mo 2(a) (0,0,0) Si 4(e) $(0,0,\frac{1}{3})$	Mo origin: 8 Si Si origin: 4Mo+4Si
$NiTi_2$	Cubic	$Fd\bar{3}m$	96	$a = 21.398$	Ni 32(e) (x', x', x') Ti 16(c) $(\frac{1}{8}, \frac{1}{8}, \frac{1}{8})$ Ti 48(f) $(x, 0, 0)$ $x' = 0.912$ $x = 0.311$	Ni (e) origin: 6Ti(f)+3Ti(c) +3Ni(e) Ti(c) origin: 6Ti(f)+6Ni(e) Ti(f) origin: 8Ti(f)+4Ni(e) +2Ti(c)

2.2. Method

The relative structural stability of the three different ($MoPt_2$- $MoSi_2$- and $NiTi_2$-type) structures is studied using a total energy approach based on the local-density approximation (LDA) [5, 6], namely the self-consistent linear-muffin-tin-orbital (LMTO) [7] method, including the combined correction terms [8] in the atomic-sphere approximation (ASA) [9]. This means that the unit cell is divided into overlapping spheres and, inside these spheres, the potential is assumed to be spherically symmetric. We include basis sets up to $l = 2$ (i.e. d orbitals) and treat the valence electrons scalar relativistically. The total energies are calculated for varying volumes in order to locate the equilibrium volume. The calculations are considered to converge when the deviation between the input and output potential is less than 0.01 mRyd. To evaluate integrals over the Brillouin zone, we use a uniform mesh of sampling points which ensure that the total energy converges to within 0.05 mRyd per atom. Since the total energies for the pure metals are treated in the same way, the formation energy is obtained by subtracting the weighted sum of total energies of the constituent elements from the total energy of the compound (i.e. $\Delta E = E_{A_mB_n} - (mE_A + nE_B)$). Hence ΔE represents the released energy when the compound is formed, which relates to the stability of the compounds.

However, some comments have to be made on the sensitivity of ΔE values with respect to the choice of the sphere radii. Indeed, it is well known that there may be problems with the ASA concerning the comparison between different structures, which is the purpose of our study. In the ASA, the non-spherical parts of the potential, the higher partial waves and the interstitial region are neglected. The ASA is a reasonable approximation provided that there are very few electrons in the interstitial region, or rather, that the touching muffin-tin spheres can be substituted by overlapping Wigner–Seitz (WS) spheres which fill the electron-containing parts of space but do not overlap more than about 30 per cent into any one sphere, i.e. $S_{R'} + S_R - |R' - R| < 0.3S_R$ for all R. However, even with these constraints, there is still some degree of freedom in the choice of the Wigner–Seitz spheres. Equal WS

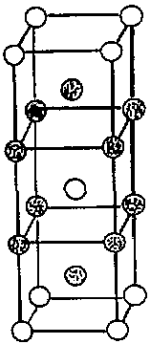

(a) *MoSi2-type* structure

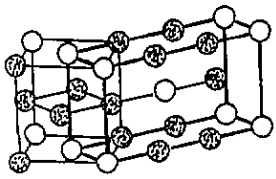

(b) *MoPt2-type* structure

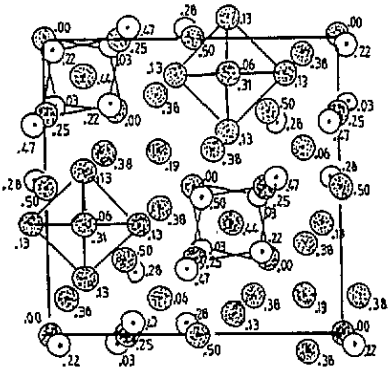

(c) *NiTi2-type* structure

Figure 1. Crystal structures. (*a*) Unit cell of the $MoSi_2$-type structure; (*b*) original FCC unit cell and unit cell of the $MoPt_2$-type structure; (*c*) simplified representation of the $NiTi_2$-type structure.

radii lead to unphysically important charge transfer between the alloy constituents when atomic volumes of both species are very different. A guiding principle for choosing the relative sphere sizes for an ASA calculation is that the radii should be chosen to be as close as possible to the atomic radii of the corresponding elemental solids [8]. This means that the net charge inside any sphere will be rather small, typically a few tenths of the charge of an electron. Experience shows that this charge neutrality is valid for most cases, like the transition metal–transition metal alloys [8]. We have used such an approach to determine WS spheres for ASA calculations of the three $MoPt_2$-, $MoSi_2$-, and $NiTi_2$-type structures. Of course, if the structure displays inequivalent crystallographic sites for A species (which is the case for Ti in the $NiTi_2$-type structure), two different A radii can be obtained within this approach. The ratio of the Ni sphere to the Ti sphere was found to be equal to 0.9 for $MoPt_2$- and $MoSi_2$-type structures. Values of 0.85 for the $r_{Ni(e)}/r_{Ti(f)}$ ratio and 0.95 for the $r_{Ti(c)}/r_{Ti(f)}$ ratio were found to be optimal for the $NiTi_2$-type structure. In order to confirm the validity of such a choice, we will compare the as-obtained ASA structural energies with the ones provided by the full-potential method [11]. In this case, the muffin-tin radii are only used to specify details of the linear basis set, i.e. the augmentation.

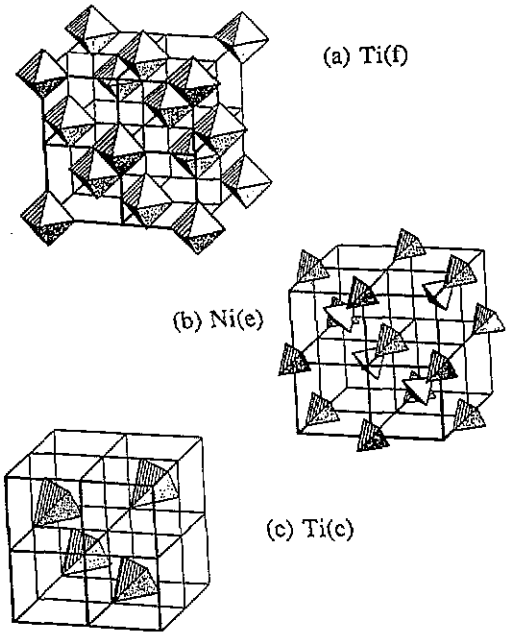

Figure 2. $NiTi_2$-type structure. (*a*) Lattice built by the Ti(f) octahedra; (*b*) lattice built by the Ni(e) tetrahedra; (*c*) lattice built by the Ti(c) tetrahedra.

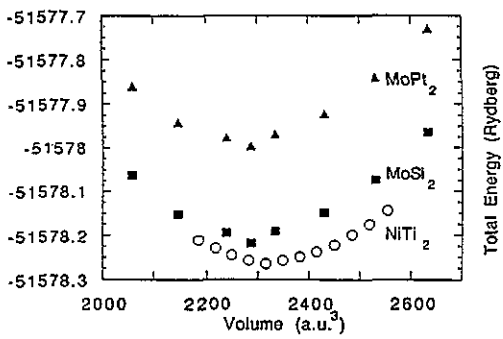

Figure 3. The scaled total energy for 24 atoms as a function of volume for the three $MoPt_2$-, $MoSi_2$- and $NiTi_2$-type structures (ASA self-consistent results).

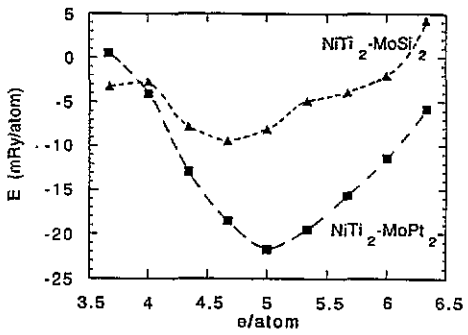

Figure 4. The energy of the $NiTi_2$-type structure relative to the $MoPt_2$- and $MoSi_2$-type structures (in mRyd/atom) as a function of the average valence electron number per atom.

2.3. $NiTi_2$ compound

The total energy versus volume is shown in figure 3 for the compound $NiTi_2$ in the three ($NiTi_2$-, $MoPt_2$-, $MoSi_2$-type) structures. The difference in the equilibrium volumes between any two of the three structures is found to be within 1%. In agreement with experiment, the $NiTi_2$-type structure has the lowest total energy among these three structures. The relative stability—$NiTi_2$, $MoSi_2$ to $MoPt_2$—remains the same, as found by full-potential LMTO calculations [11]. The calculated equilibrium cohesive properties are presented in

table 2 and compared with full-potential results. The quantitative agreement between the two sets of data is quite good but let us recall that it depends essentially on the WS radii values in the ASA calculations. The calculated lattice constant of the $NiTi_2$-type structure, $a = 11.1$ Å, is in good agreement with experiment ($a = 11.32$ Å[13]). Another point worth commenting on concerns the possibility of performing non-self-consistent total energy calculations. A positive aspect of the ASA is that the application of the force theorem becomes particularly simple [14–15], it was, for instance, used to derive the pressure relation and has been extended to a structural energy difference theorem [16]. Suppose we want the energy difference between two structures of the same composition S1 and S2. We obtain the self-consistent ASA potential for structure S1, varying the atomic-sphere radii until the spheres are neutral. Now we rearrange the atomic spheres so as to assemble the atoms in structure S2 and solve the Schrödinger equation once using the self-consistent potential parameters from structure S1. The total energy difference between the self-consistent structure S1 and structure S2 in the trial potential extracted from S1 is simply the difference in band structure energies from the two calculations. In table 2, we illustrate the procedure for the $NiTi_2$ compound, with $MoPt_2$-type as structure S1 and $MoSi_2$- and $NiTi_2$-type as structure S2. Firstly, we note that for a comparison between $MoPt_2$- and $MoSi_2$-type structures, the method is very successful. In the $NiTi_2$-type structure, Ti atoms have two symmetry-inequivalent sites and the Ni site and one Ti site have icosahedral symmetry. We also find a not so good agreement with the fully self-consistent calculations. This arises from our neglect of charge transfer calculations [17], which are certainly different in geometrically and topologically close-packed structures.

Table 2. Energy of $MoSi_2$ and $NiTi_2$ relative to the $MoPt_2$ structure (in mRyd/atom) for the $NiTi_2$ compound. Column I, ASA self-consistent calculations; column II, ASA self-consistent calculations for $MoPt_2$ phase only; column III, FP self-consistent calculations [11].

ΔE ($MoSi_2$–$MoPt_2$)			ΔE ($NiTi_2$–$MoPt_2$)		
I	II	III	I	II	III
−9.4	−10.2	−9.8	−11.4	−22.3	−13.7

2.4. Structural stability versus e/atom

Before studying the $NiTi_2$-type structure as a function of the number of valence electrons per atom, we calculated the cohesive properties of other TM–Ti_2 compounds (TM = Mn, Fe, Co). The formation energies are calculated and compared with available experimental data in table 3. The calculated formation energies are generally 20% larger than experimental ones [18] and it is necessary to perform full-potential calculations to obtain a better agreement [11]. However, ASA results give the same experimental trend, namely the $CoTi_2$ compound displays the most negative formation energy.

Table 3. Formation energies (in kJ/atom) for (Mn, Co, Fe, Ni)–Ti_2 compounds in the $NiTi_2$ structure. A comparison with experimental values [18].

	LMTO-ASA theory	Experimental values
$NiTi_2$	−35	−27
$CoTi_2$	−46	−34
$FeTi_2$	−36	−28
$MnTi_2$	−26	—

We calculated the total energy versus the electron concentration for the three different structures, varying the valence of the TM element and keeping the Ti valence constant. With the total energy of the $NiTi_2$-type structure as a reference energy, the dependence of the total energy of the $MoPt_2$- (or $MoSi_2$-)type structure on the electron concentration (e/atom) is plotted in figure 4. For e/atom between 4 and 6.5, it can be clearly seen that the $NiTi_2$-type structure is more stable than the tetragonal $MoSi_2$-type structure or the orthorhombic $MoPt_2$-type structure. In the same range, the $MoSi_2$-BCC structure is also found to be more stable than $MoPt_2$-type structure. Chemical ordering does not seem to favour the stabilization of the $MoPt_2$-type structure since for pure transition metals the FCC structure is found to be more stable than the BCC structure for e/atom between 5.2 and 7.4. This peculiar behaviour has already been observed by Turchi [10] using simple tight-binding arguments.

3. Electronic structure calculations

In order to make a connection between total energy calculations and microscopic analysis, we look at the density of states (DOS) of the $NiTi_2$ compound in its three structures (cf figures 5 and 6). We would like to point out that the $NiTi_2$-type structure is characterized by 50% atoms (types Ni and Ti(c)) which are surrounded by distorted icosahedra (CN = 12) while the other 50% atoms, i.e. Ti(f), have the coordination 14. In the $NiTi_2$-type structure (cf figure 5) two distinct regions in the DOS can be found; for energies lower than -0.2 Ryd, the valence band contains mainly Ni 3d states. At higher energies, the band structures originate essentially from Ti(c) and Ti(f) 3d states. However the positions of the two types of Ti 3d bands are not identical. From the partial DOS analysis, the Ti(f) 3d states dominate in the range -0.2 to 0.1 Ryd while the Ti(c) 3d states are preferably found in the energy range 0.1 to 0.25 Ryd. This behaviour can be explained from the stronger bonding interaction between Ni and Ti(c) 3d bands. In fact, there are only four atoms of Ni-type in the nearest-neighbour shell of Ti(f), two at a distance 2.57 Å and the other two at 2.84 Å. On the other side, the Ti(c) atom is surrounded by six nearest-neighbour Ni atoms at an average distance of 2.44 Å. The main result is a bonding–antibonding behaviour due to the hybridization between states of Ni(e) and Ti(c) sites and the occurrence of a non-bonding peak in the partial Ti(f)-3d DOS, located near the Fermi level. The DOS of the $NiTi_2$ compound in the $MoPt_2$- and $MoSi_2$-type structures are displayed in figures 6(a) and 6(b). The DOS of the $MoSi_2$-type structure resembles a two-peak structure with bonding and antibonding states. In this structure the Ti site has four Ni and four Ti atoms at 2.54 Å distance, which is just a little larger than the Ni(e)–Ti(c) distance in the $NiTi_2$-type structure. The close similarity between $MoSi_2$-type DOS and $NiTi_2$-type DOS confirms Turchi's analysis [19] that higher-order moments cannot be ignored in explaining qualitatively and quantitatively the relative stability of TCP phases in comparison with simple crystalline structures like BCC-based ones. The separation between bonding and antibonding states is less well defined in the $MoPt_2$-type structure. This is partially due to the increase of the Ni–Ti distance, i.e. 2.65 Å.

A systematic study of the DOS of TM–Ti_2 compounds (with TM = Mn, Fe, Co, Ni, Cu, Pd and Pt) in the $NiTi_2$-type structure leads to the following observations.

(i) The TM d character is found dominantly in the region below E_F, while the Ti-d states are above E_F. Now with an increase of the number of valence electrons from $MnTi_2$ to $CuTi_2$, the valence electrons occupy states up to the antibonding region, leading to a decrease of $NiTi_2$-type structure stability.

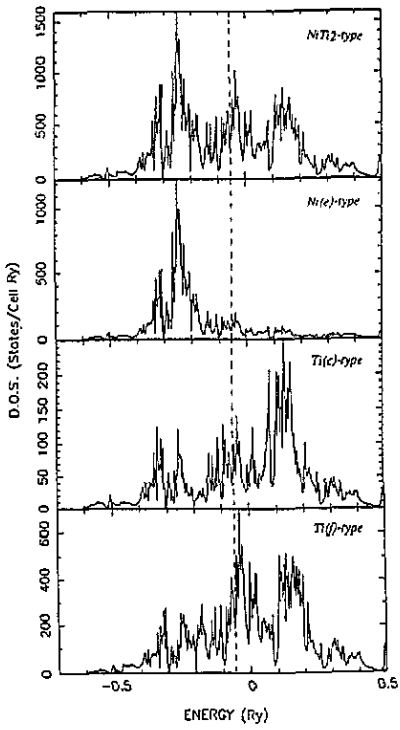

Figure 5. Total and partial DOS for the $NiTi_2$ compound in the $NiTi_2$-type structure.

(ii) Our calculations show that the hybridization effect between TM d states and Ti d states increases in going from Cu to Mn. In particular, the Ti(f) sites become more active when the TM d band filling decreases.

(iii) A study of the electronic structure of $PdTi_2$ and $PtTi_2$ compounds with 4d (Pd) and 5d (Pt) orbitals, respectively shows only very small changes in the overall shape of the DOS in comparison with that of the $NiTi_2$ compound. However, let us emphasize a relative increase of the DOS at the Fermi level, due to a weaker hybridization between 3d (Ti) states and 4d (Pd) or 5d (Pt) states.

4. Discussion

In order to confirm our analysis of the $NiTi_2$-type-structure stability, we can use LMTO–ASA calculations and the site-projected-energy analysis to obtain a local picture of the structural energies of $MoPt_2$-, $MoSi_2$- and $NiTi_2$-type structures. This approach may provide insights into the energetic factors favouring the 'good' sites and the 'bad' sites. With a potential of the atomic sphere type and if the electronic density $n(r)$ is also approximated by the spherically averaged one, we obtain the following simple so called ASA expression for the total energy per cell of the valence electrons and the ions:

$$E_{\text{tot}} = T_{\text{kin}} + \sum_R U_R + \sum_R \sum_{R'}{}' Z_R Z_{R'} \sum_T |R - R' - T|^{-1} \qquad (1)$$

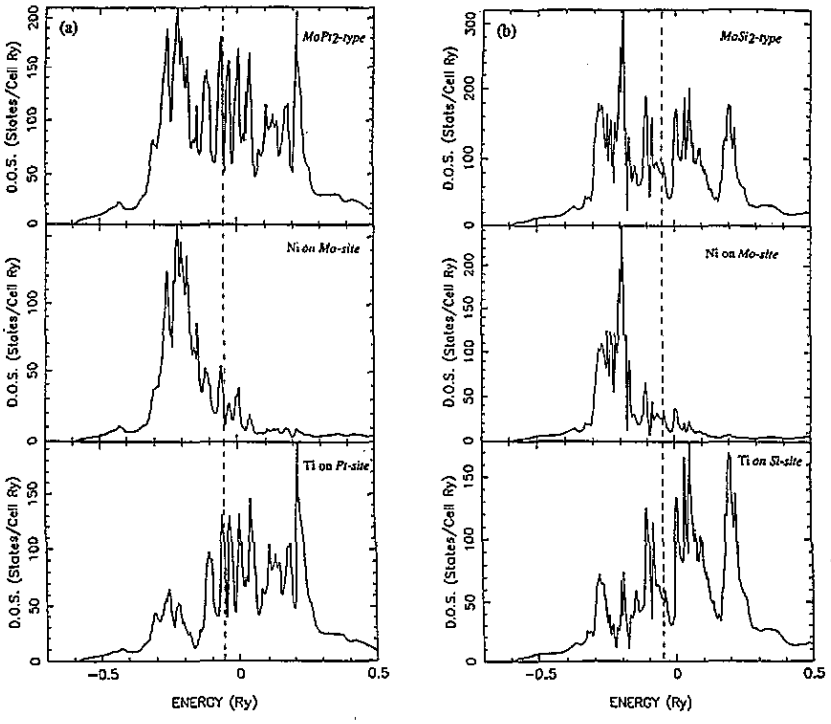

Figure 6. Total and partial DOS for the $NiTi_2$ compound in the $MoPt_2$(a)- and $MoSi_2$(b)-type structures.

where the first term is the kinetic energy, which should be expressed as the difference between the total energy and the potential energy of the non-interacting electrons. In the ASA, therefore

$$T_{\text{kin}} = \int^{E_F} EN(E)\,\mathrm{d}E - \sum_R \int_0^{s_R} v_R(r) n_R(r) 4\pi r^2\,\mathrm{d}r = \sum_R T_R \qquad (2)$$

where $N(E) = \sum_{Rl} N_{Rl}(E)$ is the sum of the projected density of states, $v_R(r)$ is the one-electron potential in the sphere at R and $n_R(r)$ the spherically averaged charge density. The second term in equation (1) is the sum of the intra-sphere interactions between the electrons and the nucleons in that sphere. The third term is the inter-sphere Coulomb (or Madelung) energy. Here z_R is the nuclear minus the electronic charge in the sphere at R. Equation (1) has thus proved useful for self-consistent calculations of the total site-projected energies in the cell and we use it in this work to investigate a local picture of the structural energies. Of course, all these results depend on the choice of the WS radii, as already mentioned in the previous sections.

In table 4, we present the results of projected-site energies for the TM(e) site (TM = Mn, Fe, Co, Ni), Ti(c) and Ti(f) sites in the $NiTi_2$-type structure. Our energies are calculated relative to the corresponding site energies in pure metals and in $MoPt_2$- and $MoSi_2$-type structures. There are some important observations which can be extracted from table 4.

(i) In the $NiTi_2$-type structure, the analysis of TM sites reveals that all of them have a more positive site-projected energy than those calculated in the corresponding pure metals

Table 4. Site-projected energies (in Ryd) of the three different types of atom in the $NiTi_2$ structure, relative to the corresponding energies in pure metals, in $MoPt_2$ or in $MoSi_2$ structures.

Site	ΔE (Ryd/atom)	$NiTi_2$	$CoTi_2$	$FeTi_2$	$MnTi_2$
TM	Pure TM	0.141 54	0.122 78	0.148 10	0.165 97
(Ni, Co, Fe, Mn)	$MoPt_2$	0.087 85	0.070 21	0.056 11	0.043 21
	$MoSi_2$	0.075 66	0.060 35	0.058 34	0.053 30
Ti(c)	Pure Ti	−0.162 54	−0.156 30	−0.141 35	−0.110 85
	$MoPt_2$	−0.111 19	−0.100 35	−0.083 06	−0.052 74
	$MoSi_2$	−0.091 01	−0.078 19	−0.062 29	−0.037 28
Ti(f)	Pure Ti	−0.095 65	−0.100 01	−0.107 00	−0.112 86
	$MoPt_2$	−0.044 30	−0.044 06	−0.048 71	−0.054 75
	$MoSi_2$	−0.024 12	−0.021 90	−0.027 94	−0.039 29

or in the two other structures. Thus, the TM sites can be considered as the 'bad' ones in favouring the $NiTi_2$-type structure.

(ii) On the contrary, we have found that all of the Ti sites are favourable ones, which ensures the stability of the $NiTi_2$-type structure. For the $NiTi_2$ compound, Ti(c) sites with an icosahedral environment gain more energy in comparison with Ti(f) sites but for the $MnTi_2$ compound, the two sites provide the same energetic contribution. From the DOS analysis discussed in the previous section, it has been shown that the alloying process in these compounds is due the coupling of Ti d states with TM d states. Classically, the d band of Ti is considered to be located above the d band of Mn, Fe, Co, or Ni [20]. By hybridization effects, the d bands of both metals adopt the same bandwidth and the consequence is that Ti gains energy while Mn, or Ni, displays the opposite behaviour. This explains why Ti sites gain energy when we compare Ti sites in TM–Ti_2 compounds with Ti sites in pure Ti. As the hybridization effects depend on the local symmetry of the sites, these effects can be more or less increased; then we can explain the difference in energy between Ti sites in $MoPt_2$-, $MoSi_2$- or $NiTi_2$-type structures. This conclusion does not agree with arguments used by Phillips *et al* [21] to discuss the stability of improved TM–Mn quasicrystal models. Indeed, they have found that the instability of their quasicrystal models is due to unfavourable Ti sites located in a glue region between large icosahedral clusters. However, all their tight-binding calculations are based on a value of the splitting between the Ti and Mn d states equal to −1 eV, which locates Ti d states below Mn d states. In order to clarify the validity of such a choice, we have used a tight-binding Hamiltonian which is directly analogous to the first-order LMTO Hamiltonian [22]:

$$H_{ij} = \bar{C}_i \delta_{ij} + \bar{\Delta}_i^{1/2} \bar{S}_{ij} \bar{\Delta}_j^{-1/2} \tag{3}$$

where $\bar{C}$ and $\bar{\Delta}$ are potential parameters in the tight-binding representation and $\bar{S}$ is the corresponding structure constant. $\bar{C}_l$ determines the centre of the l-band while $\bar{\Delta}_l$ is related to its width. All these parameters are related to the orthogonal parameters C_l, Δ_l, Q_l obtained from self-consistent LMTO–ASA band-structure calculations by the following relations:

$$(\bar{C}_l - E_l)/(C_l - E_l) = \bar{\Delta}_l^{1/2}/\Delta_l^{1/2} = 1 - (Q_l - \bar{Q}_l)(C_l - E_l)/\Delta_l \tag{4}$$

where $\bar{Q}_l$ (= 0.3485, 0.053 03, 0.010 71) is the site-independent set of s, p, d screening constants in our LMTO equations. The calculated parameters $\bar{C}_l$ and $\bar{\Delta}_l$ for two representative

compounds $NiTi_2$ and $MnTi_2$ are presented in table 5. It is important to remember that the diagonal elements of the structure factor matrix $\bar{S}_l$ have not vanished and they depend on the local environment. We have estimated these contributions to the one-site energies $\bar{C}_l$ and have found that they are negligible. The results of this table may serve to build the TB Hamiltonian for $NiTi_2$-relative structures and, for instance, we can extract the difference between the d-site energies of Ti and Mn atoms. These values are $\Delta E = E^{\mathrm{d}}_{\mathrm{Ti}} - E^{\mathrm{d}}_{\mathrm{TM}} = 3.48$ eV and 1.67 eV for $NiTi_2$ and $MnTi_2$ compounds, respectively. We note that the second value is in contradiction with $\Delta E = -1$ eV used by Phillips *et al* in their TB calculations [21], and we can explain our different conclusions obtained in this study.

Table 5. TB Hamiltonian parameters for $NiTi_2$ and $MnTi_2$ compounds deduced from the self-consistent LMTO potentials.

$NiTi_2$	Ni		Ti(c)		Ti(f)	
	$\bar{C}_l$	$\sqrt{\bar{\Delta}_l}$	$\bar{C}_l$	$\sqrt{\bar{\Delta}_l}$	$\bar{C}_l$	$\sqrt{\bar{\Delta}_l}$
4s	−0.334	0.415	−0.141	0.376	−0.191	0.362
4p	0.479	0.285	0.346	0.225	0.259	0.224
3d	−0.207	0.091	0.057	0.157	0.041	0.162
$MnTi_2$	Mn		Ti(c)		Ti(f)	
	$\bar{C}_l$	$\sqrt{\bar{\Delta}_l}$	$\bar{C}_l$	$\sqrt{\bar{\Delta}_l}$	$\bar{C}_l$	$\sqrt{\bar{\Delta}_l}$
4s	−0.171	0.427	−0.142	0.390	−0.176	0.365
4p	0.663	0.280	0.379	0.234	0.289	0.228
3d	−0.052	0.119	0.082	0.161	0.059	0.162

5. Conclusion

In this paper, we have studied the stability of the $NiTi_2$-type structure by means of first-principles calculations. Among the three different ($MoPt_2$-, $MoSi_2$- and $NiTi_2$-type) structures, self-consistent and non-self-consistent calculations give the $NiTi_2$-type structure as the most stable for the $NiTi_2$ compound, in agreement with experiments. A site-projected-energy analysis allows us to show that in the $NiTi_2$-type structure, the Ti site with icosahedral symmetry is a favourable site for stabilization. We have shown that empirical tight-binding parameters used in this study of the stability of TM–Mn quasicrystal models do not agree with our first-principles tight-binding parameters obtained for the $NiTi_2$-type structure. However, it is not sure that our first-principles tight-binding parameters are easily transferrable and that the $NiTi_2$-type structure can be used as an approximation for TM–Ti quasicrystals. Nevertheless, we believe that our calculated site-projected energies may serve as a guide in the study of the electronic origin of TM–TM quasicrystal stability.

References

[1] Watson R E and Bennett L H 1984 *Acta Metall.* **32** 477
[2] Fukunaga T, Watanabe W and Suzuki K 1984 *J. Non-Cryst. Solids* **61–62** 343
[3] Zhang Z, Ye H K and Kuo K H 1985 *Phil. Mag.* A **52** L49
[4] Dong C, Hei Z K, Wang L B, Song Q H, Wu Y K and Kuo K H 1986 *Scr. Metall.* **20** 1155

[5] Hohenberg P C and Kohn W 1964 *Phys. Rev.* **136** B 864
[6] Kohn W and Sham L J 1965 *Phys. Rev.* **140** A 1133
[7] Andersen O K 1975 *Phys. Rev.* B **12** 3060
[8] Andersen O K 1984 *Electronic Structure of Complex Systems* ed P Phariseau and W M Temmerman (New York: Plenum) p 11
[9] Andersen O K 1973 *Solid State Commun.* **13** 133
[10] Turchi P E A 1984 *Thèse de Doctorat d'Etat* Université Pierre et Marie Curie p 51
[11] Nguyen Manh D, Pasturel A, Paxton A T and van Schilfgaarde M 1993 *Phys. Rev.* B **48**
[12] Villars P and Calvert L D 1985 *Pearson's Handbook of Crystallographic Data for Intermetallic Phases* (Ohio: ASM)
[13] Mueller M H and Knott H W 1963 *Trans. Met. Soc. AIME* **227** 674
[14] Pettifor D G 1978 *J. Chem. Phys.* **69** 2930
[15] Andersen O K, Skriver H L, Nohl H and Johansson B 1980 *Pure Appl. Chem.* **52** 93
[16] Christensen N E 1986 *Phys. Rev.* B **32** 207
Christensen N E and Christensen O B 1986 *Phys. Rev.* B **33** 4739
[17] van Schilfgaarde M, Paxton A T, Pasturel A and Methfessel M 1991 *Mater. Res. Soc. Symp. Proc.* **186** 107
[18] de Boer F R, Boom R, Mattens W C M, Miedema A R and Niessen A K 1988 *Cohesion and Structure* vol 1, ed F R de Boer and D G Pettifor (Amsterdam: North-Holland)
[19] Turchi P E A 1991 *Mater. Res. Soc. Symp. Proc.* **206** 265
[20] Ducastelle F 1991 *Cohesion and Structure* vol 3, ed F R de Boer and D G Pettifor (Amsterdam: North-Holland)
[21] Phillips R, Deng H, Carlsson A E and Daw M S 1991 *Phys. Rev. Lett.* **67** 3128
[22] Andersen O K and Jepsen O 1984 *Phys. Rev. Lett.* **53** 2571